ISSN 0023-1584, Kinetics and Catalysis, 2007, Vol. 48, No. 2, pp. 214–220. © MAIK "Nauka/Interperiodica" (Russia), 2007.
Original Russian Text © Published in Russian in Kinetika i Kataliz, 2007, Vol. 48, No. 2, pp. 230–236.

Using TiO_2 Supported on Clinoptilolite as a Catalyst for Photocatalytic Degradation of Azo Dye Disperse Yellow 23 in Water[1]

M. Nikazar[a], K. Gholivand[b], and K. Mahanpoor[c]

[a] *Department of Chemical Engineering, Amirkabir University of Technology, (Center of Excellence for Petrochemicals), Tehran, Iran*

[b] *Faculty of Science, Department of Chemistry, University of Tarbiat Modares, Tehran, Iran*

[c] *Department of Applied Chemistry, Faculty of Chemistry, Islamic Azad University, North Tehran Branch, Tehran, Iran*

e-mail: kazem_mahanpoor@yahoo.com

Received August 29, 2005; in final form, May 24, 2006

Abstract—In this investigation photocatalytic degradation of azo dye Disperse yellow 23 in water was studied. Titanium (IV) oxide was supported on Clinoptilolite(CP) (Iranian Natural Zeolite) using the solid-state dispersion (SSD) method. The results show that the TiO_2/Clinoptilolite (SSD) is an active photocatalyst. The maximum effect of photo degradation was observed at 10 wt % TiO_2, 90 wt % Clinoptilolite. A first order reaction with k = 0.0119 min^{-1} was observed. The effects of some parameters such as pH, amount of photocatalyst, and the initial concentration of dye were examined.

DOI: 10.1134/S002315840702005X

INTRODUCTION

From the viewpoint of green chemistry, the photocatalytic decomposition of organic compounds in wastewater and the gas phase has attracted a great deal of attention [1–9]. TiO_2 is one of the most effective photocatalysts because it is biologically and chemically inert and photostable with near-UV band gap energy. TiO_2 can be used in the form of a fine powder or crystals dispersed in water wastewater treatment applications. However, the need to filter TiO_2 after the reaction makes such a process troublesome and more costly. Thus, in order to solve this problem, many researchers have examined methods for fixing TiO_2 on supporting materials including glass beads [10–12], fiberglass [13–15], silica [16, 17], and zeolite [18, 19]. When using zeolite as a support for TiO_2, care should be taken that TiO_2 does not lose its photo activity and that the adsorption properties of zeolite are not affected. Mattews [11] showed the photo efficiency of TiO_2 is suppressed when Ti is in interaction with the zeolite. In this work TiO_2 was supported on zeolite without losing photo efficiency and affecting the adsorption properties of zeolite. This mixture was used for degradation of aqueous Disperse yellow 23.

[1] This text was submitted by the authors in English.

EXPERIMENTAL

Materials

The titanium dioxide used was Degussa P-25 with a crystallographic mode of 80% anatase and 20% rutile, a BET surface area of 50 $m^2\ g^{-1}$, and an average particle size of 30 nm (according to the manufacturer's specifications), and the raw zeolite material was an Iranian commercial clinoptilolite (CP) (Afrand Tuska Company, Iran) from deposits in the region of Semnan. According to the supplier specification, it contains about 90 wt % CP (based on XRD internal standard quantitative analysis) and the Si/Al molar ratio is 5.78. The concentration of Fe_2O_3, TiO_2, MnO, and P_2O_5 impurities were reported to be 1.30, 0.30, 0.04, and 0.01 wt %.

The azo dye, Disperse yellow 23 (DY 23), was obtained from the company Rang Azar (Iran) and used without further purification. The molecular structure of DY 23 is shown in scheme.

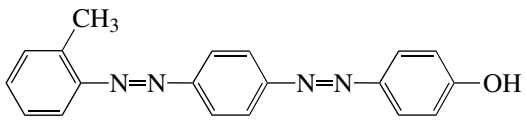

Molecular Structure of Disperse yellow 23.

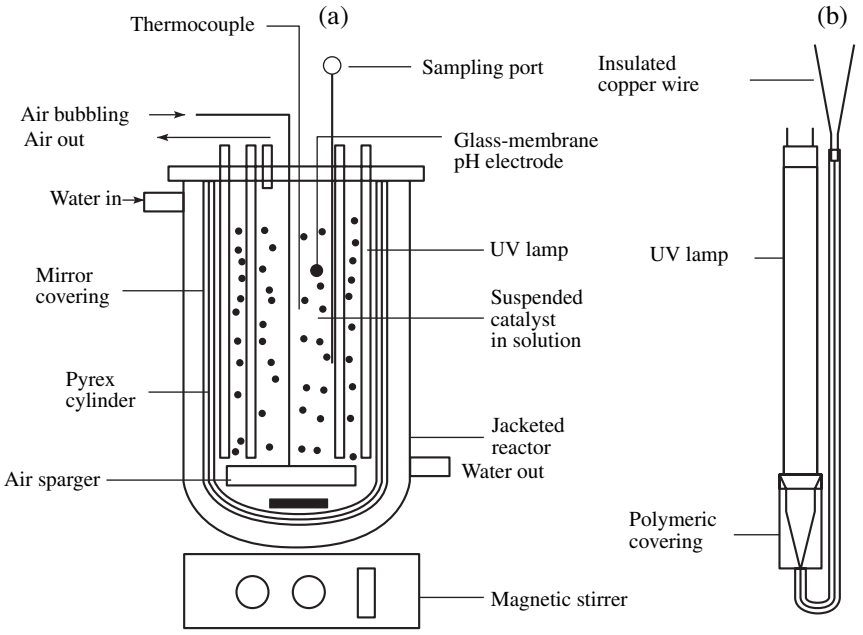

Fig. 1. Schematic diagram of the batch photocatalytic reactor (cross section view) (a), and LV lamp immersed directly in an aqueous solution (b).

Preparation of TiO_2-Supported CP Catalysts

The solid state dispersion (SSD) method was used for preparing the Zeolite-based photocatalyst. In this method, TiO_2 was mixed with zeolite using ethanol as a solvent with an agate pestle and mortar; the solvent was then removed by evaporation. Samples prepared by this method were dried at 110°C and calcined in air at 450°C for 5 h to obtain TiO_2-supported zeolite catalysts.

Apparatus

For the UV/photocatalyst process, irradiation was performed in a batch photoreactor of 2 l in volume with four mercury lamps Philips 8W (UV-C). A magnetic stirrer was used to ensure complete mixing in the tank (stirring speed = 250 rpm), and air was dispersed at a flow rate of 1 l/min by using an air diffuser to supply oxygen for the enhancement of photooxidation (Fig. 1).

A UV/VIS Spectrophotometer (Shimadzu 160A) was employed for absorbance measurements using silica cells of path length 1 cm. XRD analysis of the samples was done using a D-500 diffractometer (Siemens). BET surface areas of CP and TiCVCP were measured in an all-glass high vacuum system by N_2 adsorption at 77 K. The morphology of the resultant pure and loaded TiO_2 was obtained with a transmission electron microscope (TEM; JEM-2000FX, Japan).

Procedures

For the photodegradation of DY 23, a solution containing a known concentration of dye and photocatalyst was prepared and was allowed to equilibrate for 30 min in darkness. The suspension pH values were adjusted to the desired level using dilute NaOH and H_2SO_4 (the pH values were measured with a Horiba M12 pH meter). The photodegradation reaction took place under the radiation of a Mercury lamp, while agitation was maintained to keep the suspension homogeneous. The concentration of the samples was determined using a spectrophotometer (UV/VIS Spectrophotometer, Shimadzu 160A) at λ_{max} = 478 nm. The samples were filtered before the UV-vis spectroscopy to remove the photocatalyst. The degree of photodegradation (x) as a function of time is given by

$$x = \frac{C_0 - C}{C_0}, \quad (1)$$

where C_0 and C are the concentration of the dye at $t = 0$ and t, respectively.

RESULTS AND DISCUSSION

VV-Vis Spectra

The absorbance of DY 23 solutions during the photocatalytic process at the initial time and after 2.5 h irradiation time versus λ are shown in Fig. 2. The spectrum of DY 23 in the visible region exhibits a main band with a maximum at 478 nm. The decrease of absorption peaks of DY 23 at λ_{max} = 478 nm in this figure indicates a rapid degradation of the azo dye. Complete discoloration of the dye was observed after 3 h under optimum conditions.

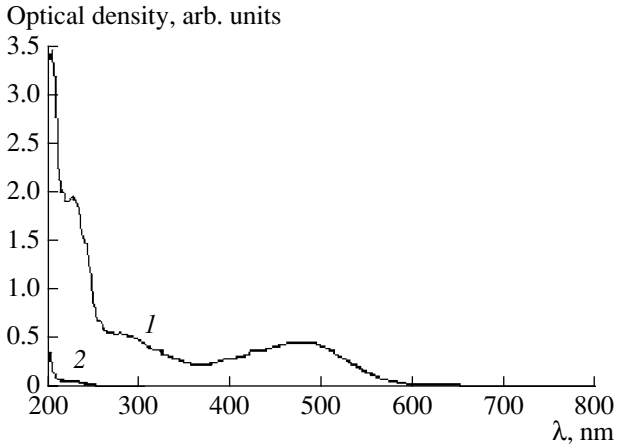

Fig. 2. UV-Vis spectra of DY 23 (20 ppm) in aqueous photocatalyst (TiO_2 10% + Clinoptilolite 90%) dispersion with concentration of 40 ppm, irradiated with a mercury lamp light at pH 7, T = 298 K, at: (*1*) t = 0, (*2*) t = 2.5 h.

Effect of VV Irradiation and Photocatalyst-employed Particles

The effects of UV irradiation, TiO_2, and the presence of CP on the photodegradation of DY 23 are shown in Fig. 3. Figure 3 indicates that, in the presence of mixed photocatalyst (10% TiO_2 and 90% clinoptilolite) and UV irradiation, 97.4% of the dye was degraded at an irradiation time of 2 h, while the amount was 63.2% for TiO_2 (without clinoptilolite) and UV irradiation. This was contrasted with 8% degradation for the same experiment performed in the absence of TiO_2, and 10.5% when the UV lamp was switched on and the reaction was allowed to occur in the presence of CP.

This is due to the fact that when TiO_2 is illuminated with light of $\lambda < 390$ nm, electrons are promoted from the valence band to the conduction band of the semiconducting oxide to give electron–hole pairs. The valence band (h_{VB}) potential is positive enough to generate hydroxyl radicals at the surface, and the conduction band (e_{CB}) potential is negative enough to reduce molecular oxygen. The hydroxyl radical is a powerful oxidizing agent and attacks organic pollutants present at or near the surface of TiO_2. It causes photooxidation of the dye according to the following reactions [11–13]:

$$TiO_2 + h\nu \longrightarrow TiO_2(e^-_{CB} + h^+_{VB}), \quad \text{(I)}$$

$$h^+_{VB} + H_2O_{ads} \longrightarrow H^+ + {}^{\cdot}OH_{ads}, \quad \text{(II)}$$

$$h^+_{VB} + OH^-_{ads} \longrightarrow {}^{\cdot}OH_{ads}, \quad \text{(III)}$$

$$e^-_{CB} + O_{2ads} \longrightarrow {}^{\cdot}O^-_{ads}, \quad \text{(IV)}$$

$${}^{\cdot}OH_{ads} + \text{dye} \longrightarrow \text{degradation of the dye}, \quad \text{(V)}$$

$$h^+_{VB} + \text{dye} \longrightarrow \text{dye}^{\cdot+} \longrightarrow \text{degradation of the dye}. \quad \text{(VI)}$$

The mechanism is summarized in Fig. 4.

Effect of the Composition of the Supported Photocatalyst

The effect of the ratio of TiO_2/CP on DY 23 removal is shown in Fig. 5. The effective decomposition of DY 23 after 120 min irradiation time was observed when the photocatalyst contained 10% TiO_2 and 90% CP, prepared by using the solid state dispersion (SSD) method.

To comment on this result, we propose that the ${}^{\cdot}OH$ (hydroxyl radical) on the surface of TiO_2 is easily transferred onto the surface of zeolite. This means the organic pollutants, which have already been adsorbed on the nonphotoactive zeolite, have a chance to be degraded due to the appearance of ${}^{\cdot}OH$, resulting in the

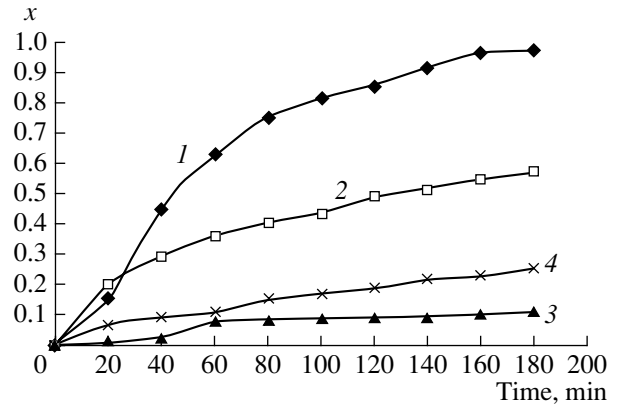

Fig. 3. Effect of UV light and different photocatalyst on photocatalytic degradation of DY 23. $|DY\ 23|_0$ = 20 ppm, photocatalyst (10% TiO_2 + 90% clinoptilolite) concentration = 40 ppm, T = 298 K, pH 7. (*1*) Irradiation in the presence of 10% TiO_2 + 90% clinoptilolite, (*2*) irradiation in the presence of TiO_2, (*3*) UV irradiation alone, and (*4*) irradiation in the presence of clinoptilolite.

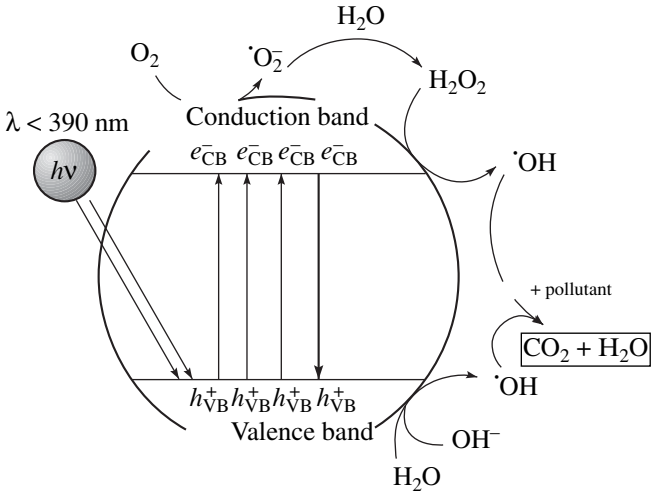

Fig. 4. General mechanism of the photocatalysis.

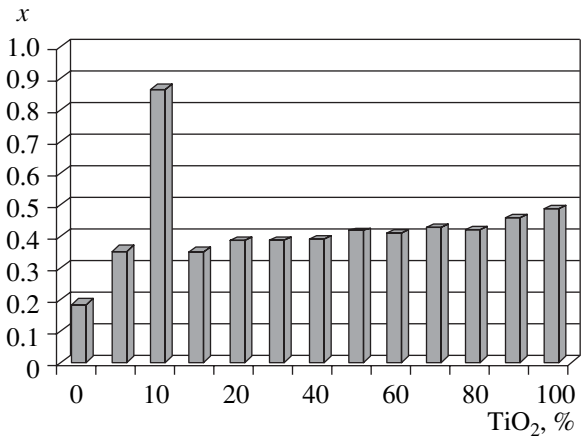

Fig. 5. Effect of composition of photocatalyst (wt % TiO_2 in mixture of TiO_2 and clinoptilolite) on photocatalytic degradation of DY 23. $[DY\ 23]_0$ = 20 ppm, concentration of photocatalyst = 40 ppm, T = 298 K, pH 7, irradiation time = 120 min.

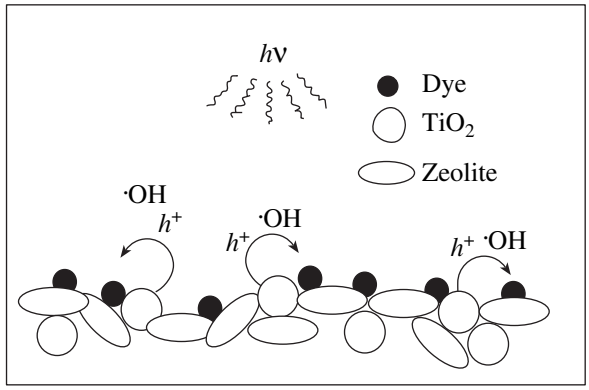

Fig. 6. Photocatalytic activity of TiO_2 + CP.

enhancement of the photodegradation performance of TiO_2–zeolite. Experimental results show that about 10 wt % of TiO_2 with respect to zeolite is the best condition to achieve the synergism between TiO_2 and CP. This synergic effect may be due to the fact that the presence of zeolite maintains the molecules of dye near the photocatalyst (local concentration effect) as depicted in Fig. 6. The enhanced photocatalytic activity over the composite TiO_2 + CP reflects the beneficial adsorption properties of CP. If the amount of TiO_2 in the composition of the photocatalyst decreases (less than 10 wt %), the rate of the $^{\cdot}OH$ production will not be enough. In this condition a few of the dye molecules that have been absorbed on the surface of zeolite can react with $^{\cdot}OH$. If the amount of TiO_2 increases in the composition of the photocatalyst (more than 10 wt %), the rate of dye absorption will not be enough. In this condition few of the $^{\cdot}OH$ can react with dye molecules.

Characterization of Photocatalysts

As is known, the pore size of clinoptilolite is 0.4–0.7 nm [19]. Figure 7 shows the TEM images of pure TiO_2 nanoparticles and TiO_2 particles loaded on the surface of CP. As can be seen, the particle size of pure TiO_2 is 30 nm or so, which is much larger than that of the loaded ones. Thus, TiO_2 particles are not able to enter into the pores. Therefore, we suggest that the protrusions are TiO_2 and nearly all of the TiO_2 particles have been loaded on the surface of zeolite, instead of into the pores and cavities. This situation means that the photocatalytic degradation of Disperse yellow 23 mostly takes place at the zeolite surface, but not in the pores. In addition, as shown in Fig. 1b, the small TiO_2 particles do not distribute compactly but reserve lacunas on the zeolite surface, which enable the support to show its adsorption ability.

The surface area of the CP (480 $m^2\ g^{-1}$) decreased in general on the supporting TiO_2 (BET surface area of TiO_2/CP with different TiO_2 wt % is between 285–365 $m^2\ g^{-1}$). The surface area of the TiO_2-supported zeolite may be taken as an index of the available porosity. Considering the particle sizes of TiO_2 and the sizes of CP zeolite medium pores (<1 nm), we conclude that there is no possibility of TiO_2 particles entering the zeolite pores in the SSD method of preparation.

To reveal the interaction between the TiO_2 and the zeolite, the crystal structures of the raw zeolite and TiO_2–zeolite calcined at 450°C after 5 h were measured, as shown in Fig. 8. It is clear that the XRD patterns of TiO_2 zeolite consist with the raw zeolite very well as calcined at 450°C for 5 h, and no diffraction peaks corresponding to typical TiO_2, including anatase and rutile, can be observed. Similar results have also been reported by other researchers [21, 22]. It implies that the frame structure of zeolite after TiO_2 loading was not destroyed.

Effect of Catalyst Concentration

The photodegradation efficiency increases with an increase in the amount of the photocatalyst (10% TiO_2 + 90% CP), up to a value of 40 ppm and then decreases when the catalyst concentration is increased. This trend can be explained by the fact that when all dye molecules are adsorbed on the photocatalyst, the addition of higher quantities of the photocatalyst would have no effect on the degradation efficiency. Another reason for this is supposedly the increased opacity of the suspension, brought about as a result of an excess of photocatalyst particles [14].

Effect of the Initial DY 23 Concentration

The effect of the initial concentration of DY 23 on the photodegradation efficiency is shown in Fig. 9. The photodegradation conversion of DY 23 decreases with

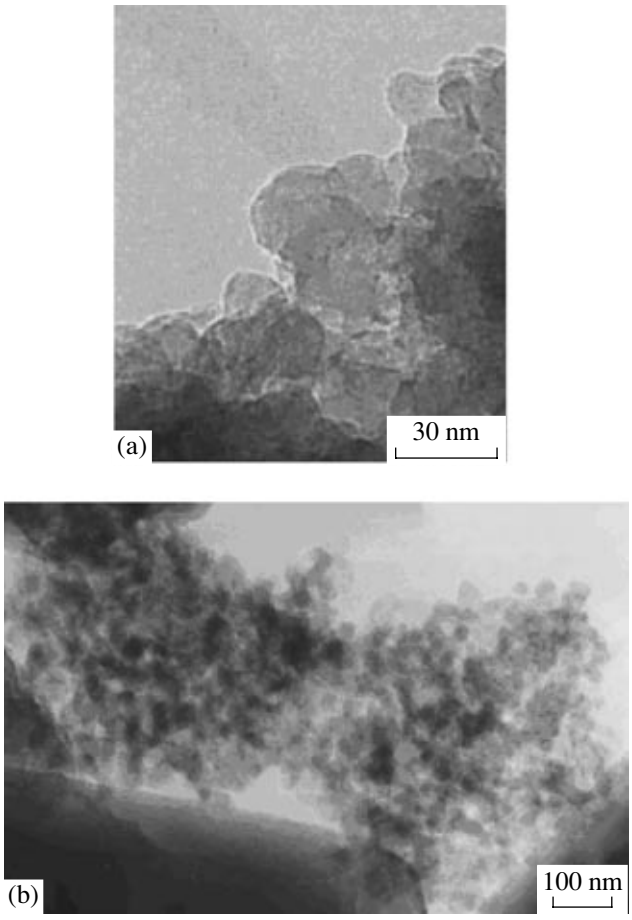

Fig. 7. TEM images of (a) pure TiO_2 nanoparticles and (b) TiO_2 particles loaded on the surface of CP.

an increase in the initial concentration of DY 23. The presumed reason is that when the initial concentration of dye is increased, more and more dye molecules are adsorbed on the surface of the photocatalyst. The large amount of adsorbed dye is thought to have an inhibitive effect on the reaction of dye molecules with photogenerated sites or hydroxyl radicals, which is due to the lack of any direct contact between them. Once the concentration of dye is increased, it also causes the dye molecules to adsorb light and the photons never reach the photocatalyst surface; thus, the photodegradation efficiency decreases.

Effect of pH

The pH is one of the main factors influencing the rate of degradation of some organic compounds in the photocatalytic process [15, 16]. It is also an important operational variable in actual wastewater treatment. Figure 10 shows the photodegradation of DY 23 at different pH from 6 to 11, which clearly shows that the best results were obtained in an alkaline solution (pH 11, $x = 100\%$). As is inferred in reaction (4), in the alkaline solutions the formation of $^{\bullet}OH$ onto photocatalyst surface is favored; thus, the photodegradation efficiency increases in the alkaline solutions for photodegradation of DY 23.

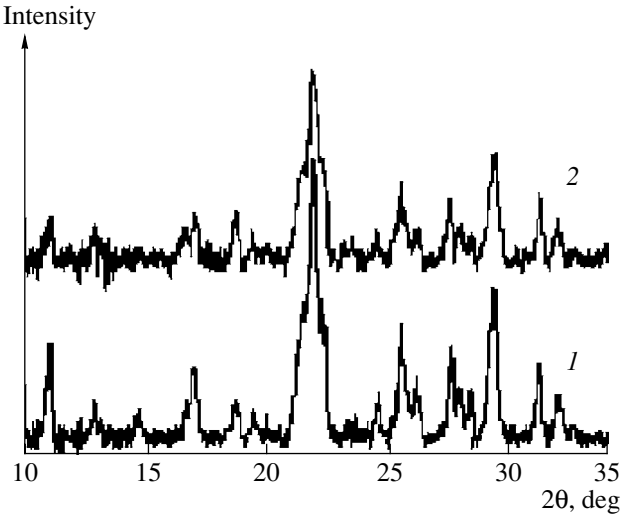

Fig. 8. XRD patterns of 10 wt % TiO_2 and 90 wt % clinoptilolite zeolite prepared by the (SSD) method after calcined in air at 450°C for 5 h (*1*) and initial clinoptilolite (*2*).

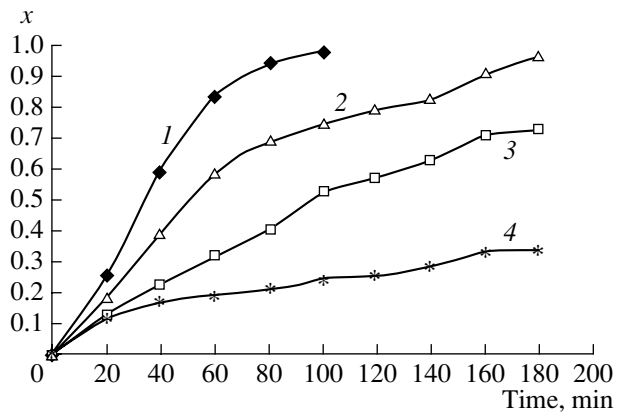

Fig. 9. Effect of initial DY 23 concentration ((*1*) 20, (*2*) 40, (*3*) 60, and (*4*) 80 ppm) on photodegradation efficiency in different time. The concentration of photocatalyst = 40 ppm, $T = 298$ K, pH 7.

Kinetics of Photocatalytic Degradation of DY 23

Several experimental results indicated that the degradation rates of photocatalytic oxidation of various dyes over illuminated TiO_2 fit by the first-order kinetic model [23–30].

Figure 11 shows the plot of Ln ($[Dye]_0/[Dye]$) versus irradiation time for DY 23. The linearity of the plot suggests that the photodegradation reaction approximately follows the pseudo–first order kinetics with a rate coefficient $k = 0.0119$ min^{-1}.

For a first order reaction, the relation of the half-time $t_{1/2}$ to the rate constant can be found from Eq. (2)

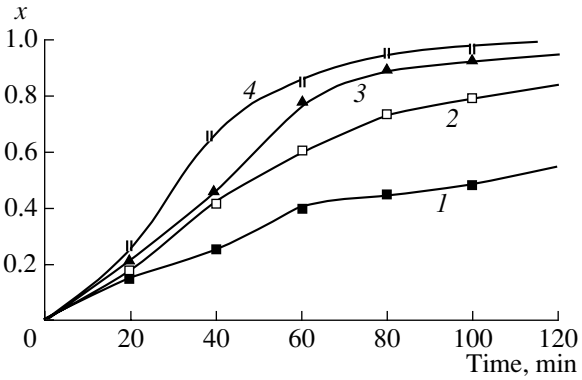

Fig. 10. Effect of pH on photodegradation efficiency of DY 23 at different irradiation times. $[DY\ 23]_0$ = 20 ppm, concentration of photocatalyst (10% TiO_2 + 90% clinoptilolite) = 40 ppm, T = 298 K. pH (*1*) 6, (*2*) 7, (*3*) 9, and (*4*) 11.

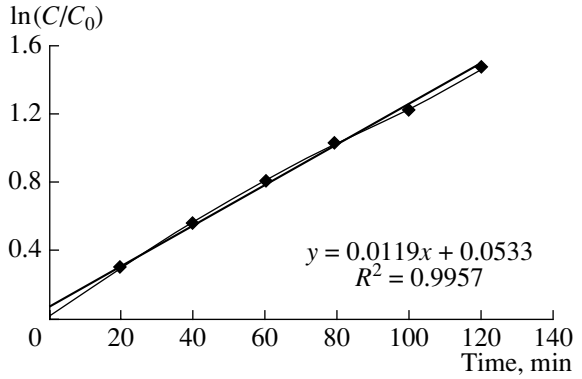

Fig. 11. Plot of reciprocal of pseudo–first order rate constant against initial concentration of DY 23 = 20 ppm, concentration of photocatalyst (10% TiO_2 + 90% clinoptilolite) = 40 ppm, T = 298 K, pH 7.

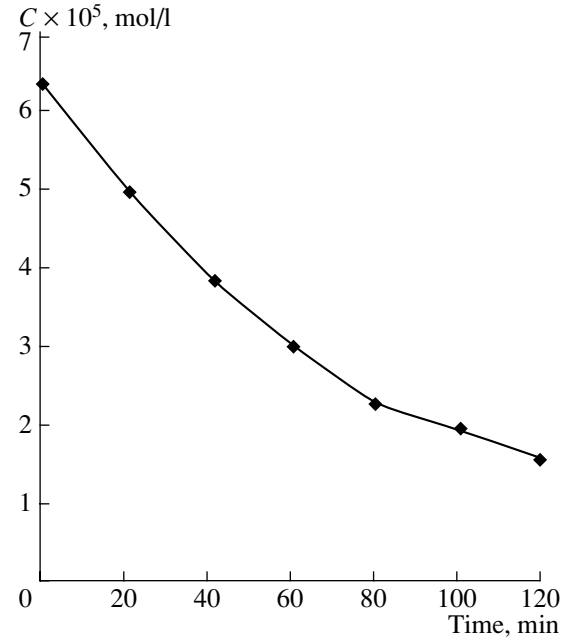

Fig. 12. Plot of dye concentration versus time: initial dye concentration = 20 ppm (6.35×10^{-5} M), concentration of photocatalyst (10% TiO_2 + 90% clinoptilolite) = 40 ppm, T = 298 K, pH 7.

by inserting the requirement that at $t = t_{1/2}$ the concentration is $C = 1/2C_0$.

$$\ln\frac{C_0}{C} = \ln\frac{C_0}{1/2C_0} = \ln 2 = kt_{1/2}. \quad (2)$$

The half-life calculated for the reaction at the concentration of DY 23 = 20 ppm (6.35×10^{-5} M), concentration of the photocatalyst (10% TiO_2 + 90% clinoptilolite) = 40 ppm, T = 298 K, and pH 7 is 58.25 min. The half-life is estimated from C-versus-t (Fig. 11). The display is in agreement with the value calculated for it. Then we can also confirm that the amount of k and the rate order (obtained from Fig. 1) is correct.

CONCLUSIONS

(1) The SSD method is an effective method for supporting TiO_2 on CP.

(2) A photocatalyst containing 10% TiO_2 and 90% CP has the maximum photodegradation efficiency of DY 23.

(3) The photodegradation conversion of DY 23 decreases with an increase in the initial concentration of DY 23.

(4) pH is one of the main affecting factors, and the optimum pH was obtained about 9–11.

(5) The kinetics of photocatalytic degradation of DY 23 is pseudo–first order with $k = 0.0119\ min^{-1}$.

ACKNOWLEDGMENTS

The authors would like to thank Dr. B. Bonakdarpour for editing the manuscript.

REFERENCES

1. Miller, R. and Fox, R., in *Photocatalytic Purification and Treatment of Water and Air*, Ollis, D.F. and Al-Ekabi, H., Eds., Amsterdam: Elsevier, 1993.
2. Vorontsov, A.V., Kozlov, D.V., Smirniotis, P.O., and Parmon, V.N., *Kinet. Katal.*, 2005, vol. 46, no. 2, p. 203 [*Kinet. Catal.* (Engl. Transl.), vol. 46, no. 2, p. 189].
3. Fox, M.A., Doan, K.E., and Dulay, M.T., *Res. Chem. Intermed.*, 1994, vol. 20, p. 711.
4. Greem, K.J. and Rudham, R., *J. Chem. Soc.*, 1993, vol. 89, p. 1867.
5. Vorontsov, A.V., Stoyanova, I.V., Kozlov, D.V., Simagina, V.I., and Savinov, E.N., *J. Catal.*, 2000, vol. 189, p. 360.
6. Aldullahm, M., Low, G.C., and Mattews, R.W., *J. Phys. Chem.*, 1990, vol. 94, p. 6820.
7. Mattews, R.W., *Water Res.*, 1990, vol. 24, p. 653.
8. Mattews, R.W., *J. Catal.*, 1988, vol. 113, p. 549.
9. Sabate, J., Anderson, M.A., Agumdo, M.A., Gimeniz, J., Cerveramarch, S., and Hill, C.G., *J. Mol. Catal.*, 1992, vol. 71, p. 57.
10. Xu, Y. and Chen, X., *Chem. Ind.*, 1990, vol. 6, p. 497.

11. Mattews, R.W., *J. Phys. Chem.*, 1988, vol. 92, p. 6853.
12. Sahate, J., Anderson, M.A., Kikkawa, H., Edwards, M., and Hill, G.G., *J. Catal.*, 1991, vol. 127, p. 167.
13. Xu, Y., Menassa, P.C., and Langford, C.H., *Chemosphere*, 1988, vol. 17, p. 1971.
14. Mattews, R.W., *Solar Energy*, 1987, vol. 38, p. 405.
15. Hofstandler, K., Kikkawa, K., Bauer, R., Novalic, C., and Heisier, G., *Environ. Sci. Technol.*, 1994, vol. 28, p. 670.
16. Anpo, M., Nakaya, H., Kodama, S., Kubokawal, Y., Domen, K., and Onishi, T., *J. Phys. Chem.*, 1986, vol. 90, p. 1633.
17. Sato, S., *Langmuir*, 1988, vol. 4, p. 1156.
18. Yoneyama, H., Hag, S., and Yamanaka, S., *J. Phys. Chem.*, 1989, vol. 93, p. 4833.
19. Breck, D.W., *Zeolite Molecular Sieves: Structure, Chemistry, and Use*, New York: Wiley, 1974, p. 29.
20. Kim, Y.I., Keller, S.W., Krueger, J.S., Yonemoto, E.H., Saupe, G.B., and Mallouk, I.E., *J. Phys. Chem. B*, 1997, vol. 101, p. 2491.
21. Kim, Y. and Yoon, M., *J. Mol. Catal. A: Chem.*, 2001, vol. 168, p. 257.
22. Chen, H., Matsumoto, A., Nishimiya, N., and Tsutsumi, K., *Colloids Surf., A*, 1999, vol. 157, p. 295.
23. Saquib, M. and Muneer, M., *Dyes Pigments*, 2003, vol. 56, p. 37.
24. Linsebigler, A.L., Guangquan, L., and Yates, J.T., *Chem. Rev.*, 1995, vol. 95, p. 735.
25. Augugliaro, V., Baiocchi, C., Bianco-Prevot, A., Garcia-Lopez, E., Loddo, V., Malato, S., Marci, G., Palmisano, L., Pazzi, M., and Pramauro, E., *Chemosphere*, 2002, vol. 49, p. 1223.
26. Stylidi, M., Kondarides, D.I., and Verykios, X.E., *Appl. Catal., B*, 2003, vol. 40, p. 271.
27. Epling, G.A. and Lin, C., *Chemosphere*, 2002, vol. 46, p. 561.
28. Shourong, Z., Qingguo, H., Jun, Z., and Bingkun, W., *J. Photochem. Photobiol., A*, 1997, vol. 108, p. 235.
29. Concalves, M.S.T., Oliveira-Campos, A.M.F., Pinto, M.M.S., Plasencia, P.M.S., and Queiroz, M.J.R.P., *Chemosphere*, 1999, vol. 39, p. 781.
30. Tanaka, K., Padermpole, K., and Hisanaga, T., *Water Res.*, 2000, vol. 34, p. 327.